

**EMISSION FROM UNBOUND STATES IN PREEQUILIBRIUM REACTIONS ($\alpha, {}^3\text{He}$)
AND (α, t) ON ${}^{197}\text{Au}$ AT $E_\alpha = 50$ MeV****A.M. Blechman¹, A. Duysebaev***Institute of Nuclear Physics, National Nuclear Center of the Republic of Kazakhstan,
480082 Almaty, Kazakhstan*

Received 23 September 1999, in final form 12 September 2000, accepted 5 October 2000

Inclusive spectra of ${}^{197}\text{Au}(\alpha, t)$ and ${}^{197}\text{Au}(\alpha, {}^3\text{He})$ reactions at $E_\alpha = 50$ MeV have been measured in a wide range of energies and angles. The results are compared with the exciton model coalescence and with the α particle elastic break-up PWBA calculations. New mechanism of formation and consequently of the emission from states with different number of unbound particles is proposed to describe the complex particle emission in α -induced reactions within the frame of the exciton model.

PACS: 25.55.-e, 25.60.Dz, 24.60.Gv

1 Introduction

Important role of structure of incident complex particle ($A > 1$) on preequilibrium cross-sections is well known [1–3]. Quantum-mechanical and semi-classical models are used in analysis of continuum energy and angular distributions. Feshbach-Kerman-Koonin [4] and other quantum approaches (e.g. [5]) are still restricted mainly to nucleon induced reactions [6, 7]. At the same time, it must be mentioned that collective excitations in continuum, analyzed in [6], would be more profoundly formed by incident complex particles due to the clusterization of the projectile [8]. The exciton model is also successful to analyze the angle-integrated spectra of some of reactions involving clusters [9, 10]. The ways how to calculate bound and unbound state densities were developed and used in calculations of statistical multistep direct (MSD) and multistep compound (MSC) processes in the frame of the exciton model [11–13]. The way of calculation of densities of states with different number of unbound particles and the possibility within this formalism which are aimed to get more adequate description of measured double-differential cross sections of (α, t) and ($\alpha, {}^3\text{He}$) reactions on ${}^{197}\text{Au}$ are shown in this work.

2 Experiment

The experiment has been performed on the isochronous cyclotron U-150M of the INP NNC of Kazakhstan with the alpha particle beam of 50.1 ± 0.5 MeV. Registration and identification

¹E-mail address: adm@burt.academ.alma-ata.su

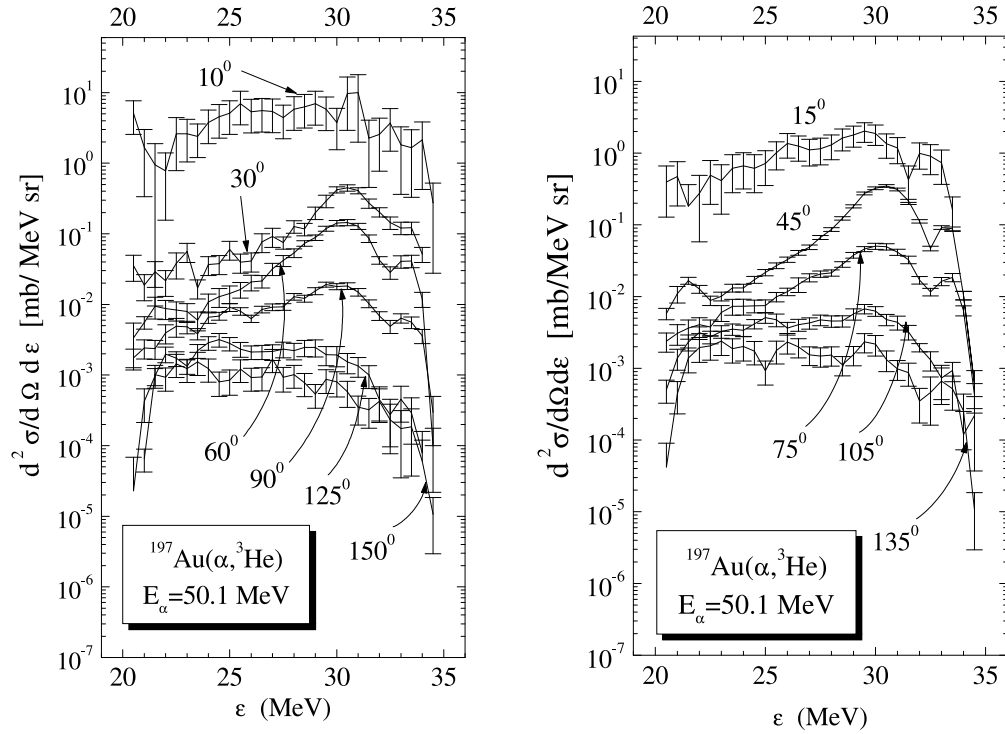


Fig. 1. (Left:) Experimental energy spectra (in the c.m. system) from the $^{197}\text{Au}(\alpha, {}^3\text{He})$ reaction at $E_\alpha = 50.1$ MeV measured at several selected angles. (Right:) The same as before, but measured at other angles.

system were based on standard $\Delta E - E$ technique with use of CsI(Tl) (for tritium) and silicon (for ${}^3\text{He}$) as stop detectors, and of silicon ($100 \mu\text{m}$ for ${}^3\text{He}$ and $200 \mu\text{m}$ for tritium) as ΔE detectors. Full energy resolution was equal to about 0.5 MeV for the ${}^3\text{He}$ measurements and 1 MeV for the tritium ones and it was mainly determined by beam resolution (≈ 400 keV). The self-supporting, isotopically enriched (99.5%) gold foils with thickness of 7.6 ± 0.7 mg/cm 2 have been used in this experiment. All measured spectra have been averaged in 1 MeV and 0.5 MeV bins for t and ${}^3\text{He}$, respectively, and then they have been transformed to the center of mass system. The angular distributions of tritium were measured in 15° to 150° range with increment of 15° , and of ${}^3\text{He}$ ions from 10° to 150° using 5° steps. Telescopes of detectors of solid angle of 4.02×10^{-6} sr (for ${}^3\text{He}$) and 27.6×10^{-6} sr (for tritium) were used.

The measured experimental spectra and angular distributions are shown in Figs. 1 to 3.

3 Analysis of experimental results

Both the ${}^3\text{He}$ and ${}^3\text{H}$ spectra measured at forward angles demonstrate wide bump with peak position about $\frac{3}{4}E_\alpha$, (where E_α is the beam energy), so that one may suggest that this bump is

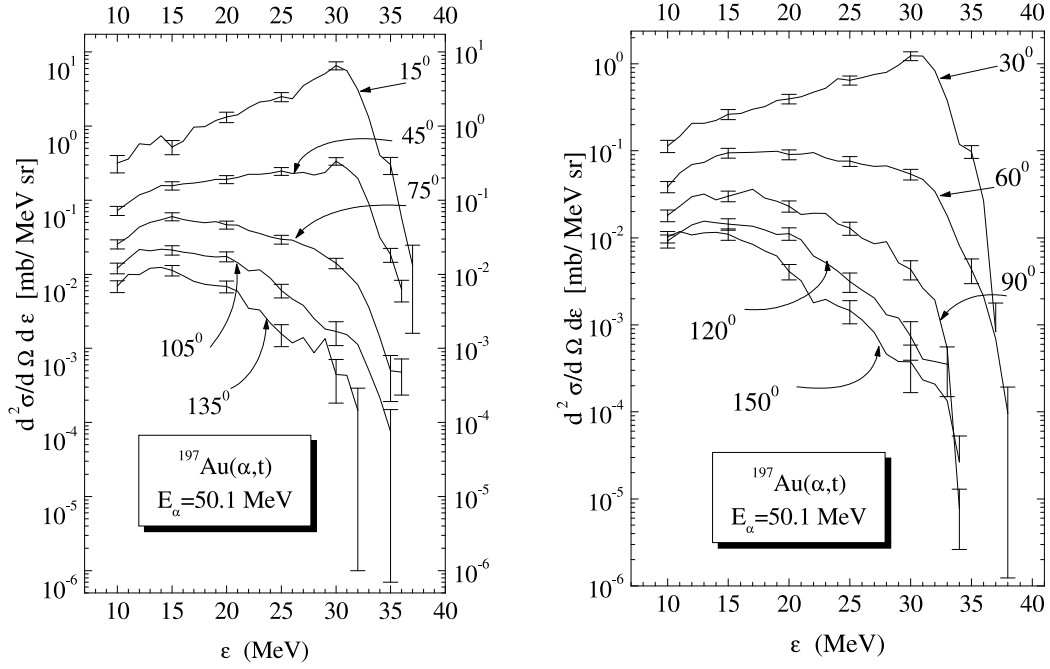


Fig. 2. The same as in Fig. 1 for the $^{197}\text{Au}(\alpha, t)$ reaction.

produced by a break-up of the incident α -particle in the field of target nucleus. One can observe a contribution from the projectile break-up process in the proton-, deuteron-, tritium- and ^3He -spectra measured in α -induced reactions [14]. This mechanism is manifested by a presence of a broad peak centered around $\frac{1}{4}mE_\alpha$ (where m is the mass number of emitted particle and E_α is the beam energy) for inclusive spectra measured at forward angles. The correlation experiments performed at incident energies close to 100 MeV confirm the existence of break-up of α particle. For an estimation of the role of this mechanism we apply a simple PWBA approach [15], used there for the description of the incident ^3He ions break-up. The calculation of corresponding break-up transition matrix is, following to [15], based on use of the Yukawa type α -particle wave function

$$\psi_\alpha(r) = C \left(\frac{\chi}{2\pi} \right)^{\frac{1}{2}} \frac{1}{r} \exp(-\chi r), \quad (1)$$

with $\chi = \sqrt{2\mu_{ti}\varepsilon_i^\alpha}/\hbar$, where μ_i ($i = t$ or $i = \tau$) is the reduced mass of the triton-plus-proton (^3He plus neutron) system and ε_i^α is the binding energy of the proton (neutron) within the α particle for the triton (^3He) emissions, respectively, C is a normalization constant. Then according to [15], the momentum \mathbf{P}_t (\mathbf{P}_τ) of emitted triton (^3He) is the sum of that due to the c.m. motion of the incident α particle (i.e., $\frac{3}{4}\mathbf{P}_\alpha$) and the internal triton (^3He) momentum \mathbf{P} within the α particle at the time of break-up. That is, $\mathbf{P}_i = \frac{3}{4}\mathbf{P}_\alpha + \mathbf{P}$. With the use of wave

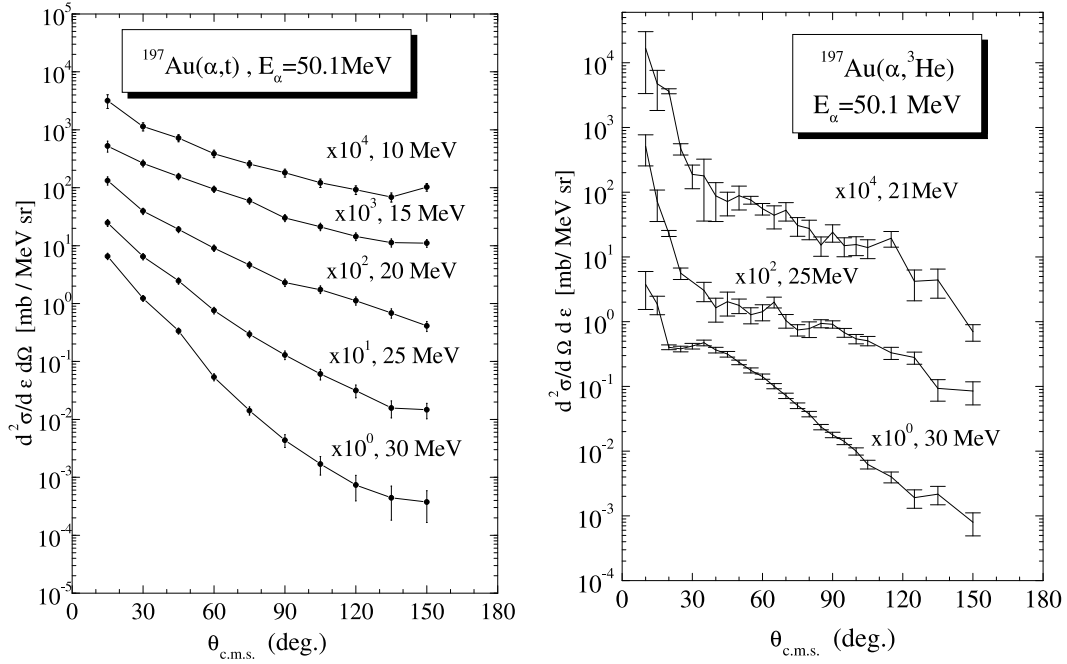


Fig. 3. Angular distributions from the $^{197}\text{Au}(\alpha, t)$ reaction (left) and from the $^{197}\text{Au}(\alpha, {}^3\text{He})$ reaction (right).

function (1) and following the approach of Ref. [15], this results in the laboratory triton energy distribution due to the α particle break-up

$$\frac{d^2\sigma}{d\Omega dE_i} \propto \frac{1}{\pi^2} m_t P_t (2\mu_{tp} \varepsilon_{tp}^\alpha)^{\frac{1}{2}} \int d\mathbf{P}_A d\mathbf{P}_p \times \frac{\delta(\mathbf{P}_t + \mathbf{P}_p + \mathbf{P}_A - \mathbf{P}_\alpha) \delta(E_t + E_p + E_A - E_\alpha + \varepsilon_{tp}^\alpha)}{[2\mu \varepsilon_{tp}^\alpha + (\frac{3}{4}\mathbf{P}_\alpha - \mathbf{P}_t)^2]^2} \quad (2)$$

and similarly for the ${}^3\text{He}$ ions. Here, m_t (m_τ) is the triton (${}^3\text{He}$) mass and E_t (E_τ) its laboratory energy. The subscript A stands for the target nucleus.

Triton and ${}^3\text{He}$ spectra calculated at 45° with the use of Eq. (2) were transformed to the c.m. system and then they have been normalized to the corresponding experimental ones. The same normalizing constants were used for the calculated 0° break-up spectra. Results of calculations compared to the experimental spectra measured at 45° are shown in the left part of Fig. 4. One can see that predicted bump of break-up spectra is shifted from $\frac{3}{4}E_\alpha$ mentioned above due to the threshold (separation energies of ${}^3\text{He}$ and triton clusters in α particle are $\varepsilon_{\tau n}^\alpha = 20.578$ MeV and $\varepsilon_{tp}^\alpha = 19.814$ MeV, respectively) relations. In order to include the Coulomb force effects at peripheral region of target nucleus, the “local” momentum values [15]

$$\mathbf{P}_\alpha^L = \mathbf{P}_\alpha \times \sqrt{1 - 4m_\alpha V_c / P_\alpha^2},$$

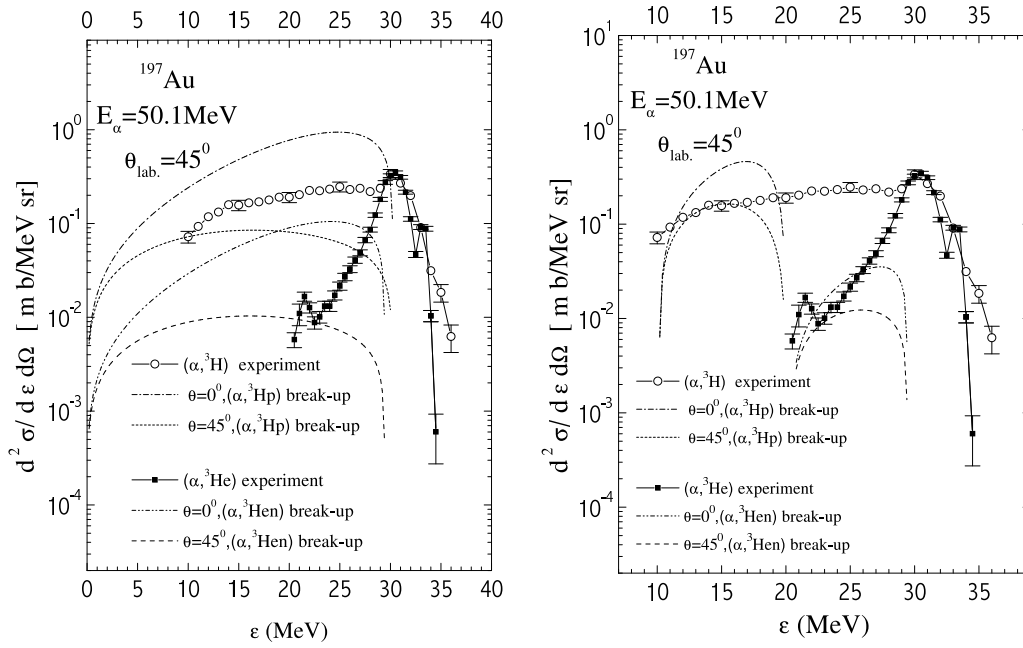


Fig. 4. Measured t and ${}^3\text{He}$ spectra from $\alpha+{}^{197}\text{Au}$ at 45° given in comparison with calculated α particle break-up energy distributions. Break-up spectra were calculated with the use PWBA approach (left) and with use of “local” momentum corrections for the incident α particle and its fragments (right). See details in the text.

$$\begin{aligned} \mathbf{P}_t^L &= \mathbf{P}_t \times \sqrt{1 - 4m_t V_c / P_t^2}, \\ \mathbf{P}_\tau^L &= \mathbf{P}_\tau \times \sqrt{1 - 4m_\tau V_c / P_\tau^2}, \end{aligned} \quad (3)$$

were used in the denominator of integral in (2) for the incident α particle and for its break-up fragments. Here V_C is the target nucleus Coulomb barrier height for proton. The results of such corrected spectra are shown in the right part of Fig. 4. Thus, one can see that the observed spectral shape of ${}^3\text{He}$ and triton emission spectra cannot be explained by the α particle break-up only. It is difficult to determine the break-up cross section because other processes may contribute to the same energy region, which cannot be distinguished from the breakup process on the basis of these inclusive data. Especially, it is true for incident α particles at energy close to 100 MeV on heavy target nuclei, where emission due to evaporation, pre-equilibrium and breakup mechanisms contribute to the same energy region. And what more, it is very difficult to distinguish the non-elastic breakup in the field of target nuclei from the multi-step processes even conceptually in this case. Thus, it is very difficult to estimate reliably the role of the elastic α particle break-up mechanism in presented spectra. On the other hand, the pre-equilibrium complex particle emission is experimentally well established, but its theoretical description is still not yet fully developed. Thus we started from pre-equilibrium model analysis.

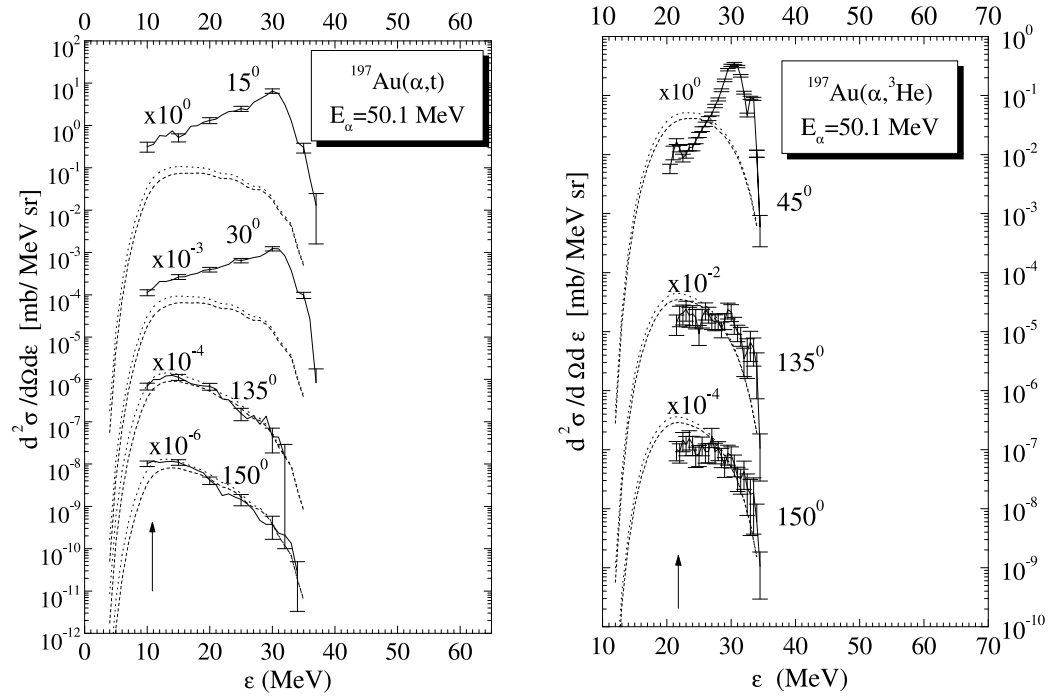


Fig. 5. Comparison of measured and calculated triton (left) and ^3He spectra (right): dotted curves stand for the assumption of spherical nuclei and the dashed lines for the deformed ones.

The measured angular inclusive spectra were compared with calculations within the exciton model [16]. The initial exciton configuration was chosen as $n_0 = (5p1h)$, using the density levels parameters from [17] for both deformed and spherical nuclei.

One can see in Fig. 5 that calculations with both sets are similar and that they reproduce the experimental spectra measured at backward angles. However, the discrepancies at forward angles are significant.

Obviously, the contribution of states of exciton number $n < 6$ ($5p1h$) is essential in the reactions $(\alpha, ^3\text{H}x)$ and $(\alpha, ^3\text{He}x)$. The initial exciton number is a parameter of the model. Thus we arrive to the necessity to use configurations of $4p0h = (2p_\pi 0h_\pi 2p_\nu 0h_\nu)$ type to reproduce the $(\alpha, ^3\text{H}x)$ and $(\alpha, ^3\text{He}x)$ spectra measured at forward angles. As an example, Fig. 6 shows the contributions from the $4p0h$ state and those from more complex states to the energy spectrum of $^{197}\text{Au}(\alpha, ^3\text{He}x)$ measured at 15° .

One can observe significant improvement of the calculated spectra at forward angles. At the same time, the form of theoretical spectra of the $^{197}\text{Au}(\alpha, t)$ reactions is not in accord with the data. Therefore, we started to study possible manifestation of the initial exciton number in the angular distributions. Such a task does not assume evaluating of the n_0 value alone, but rather a study of possible adequate description of the initial stages of the relaxation process in the present

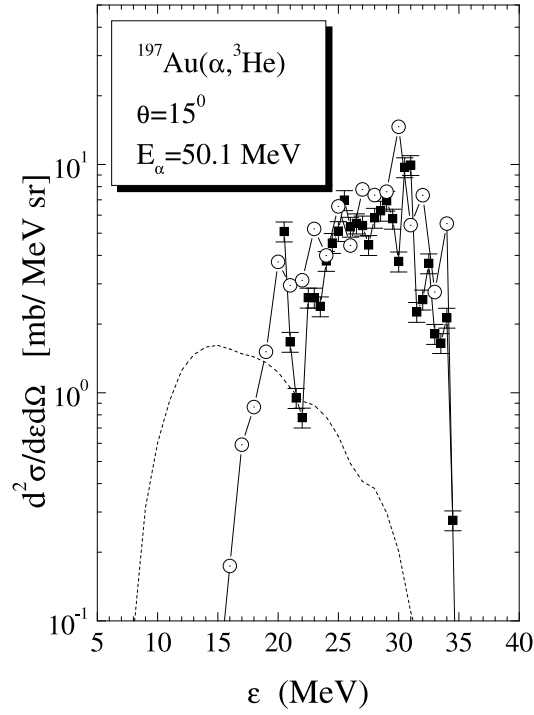


Fig. 6. Influence of different configurations on the resulting spectra of the $^{197}\text{Au}(\alpha, {}^3\text{He})$ reaction at 15° . Full points are the experimental data, full line with open points depicts the emission from the $4p0h$ state and the dashed line from $5p1h$ and more complex configurations.

versions of pre-equilibrium decay. An idea of open (unbound) and bound particles [11, 12] assumes that the particle emission occurs only from the unbound states, and the emission rate of a particle b of energy ε from unbound state (p, h, E) is

$$W_b(p, h, \varepsilon) = \frac{2s_b + 1}{\pi^2 \hbar^3} \mu_b \varepsilon \sigma_{\text{inv}}(\varepsilon) R_b(p) \frac{\omega(p - A_b, h, U)}{\omega^{(u)}(p, h, E)}. \quad (4)$$

Pre-equilibrium cluster emission has been studied in [18] under the assumption that the emitted particles are formed of the excitons above the Fermi level

$$W_b(p, h, \varepsilon) = \frac{2s_b + 1}{\pi^2 \hbar^3} \mu_b \varepsilon \sigma_{\text{inv}}(\varepsilon) R_b(p) \frac{\omega(p - A_b, h, U)}{\omega^{(u)}(p, h, E)} \gamma_b \frac{\omega(A_b, 0, E - U)}{g_b}. \quad (5)$$

Here, γ_b is the factor of clusterization of emitted particle, s_b its spin, U is the excitation energy of the residual nucleus, ε is the channel energy, E the excitation energy of the composite system and p (h) the number of exciton particles (holes); $R_b(p)$ is the factor to follow necessary isotopic composition of the emitted cluster, $\omega(p, h, E)$ is the state density of nucleus in configuration (p, h) and $\omega^{(u)}(p, h, E)$ is the density of unbound states of nucleus in that configuration.

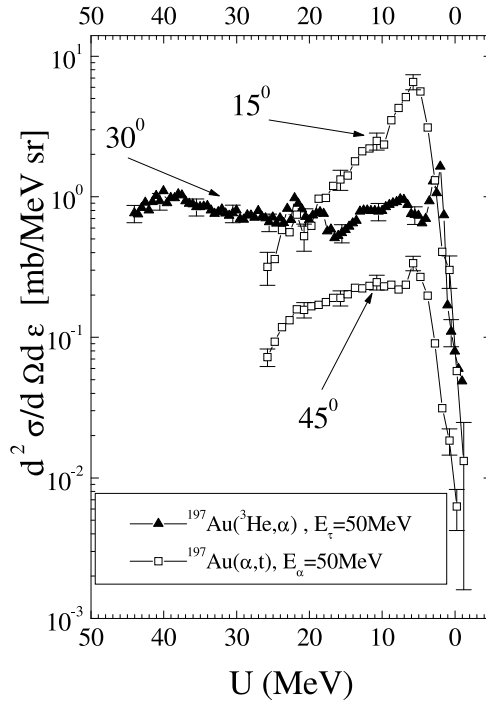


Fig. 7. Comparison of experimental spectra from the $^{197}\text{Au}(^3\text{He}, \alpha)$ reaction at 30° (full triangles) and from $^{197}\text{Au}(\alpha, t)$ at 15° and 45° , respectively (open squares), plotted versus the excitation energy of the residual nucleus U .

Spectra at forward angles are mainly defined by the emission from the few first configurations of the relaxation process in the exciton model [19] and thus the shape of spectra is connected directly to the emission rates from the initial configuration (e.g. (4) or (5)).

Let us compare the complex particle energy spectra on Au target at forward angles qualitatively. A comparison of reactions $(\alpha, ^3\text{He})$ and (α, t) allows us to study the stripping into bound and unbound states of the residual nucleus. The study of stripping processes is usually performed for isolated nuclear states [20], but in our case, with taking into account the fact of high levels density of nucleus ^{197}Au , we have stripping into continuum of bound and unbound states. Both these reactions lead to the $1p0h$ state in the residual nucleus. The spectra shown in Fig. 4 demonstrate different widths of the region of bound states of the residual nucleus, which is determined by the proton separation energy $S_p = V_p + B_p$ for the (α, t) reaction and the neutron one ($S_n = B_n$) for $(\alpha, ^3\text{He})$. Here, B_b is the separation energy and V_p is the proton Coulomb barrier.

Similar analysis will be useful for the pick-up reaction $(^3\text{He}, \alpha)$ [21, 22]. As the configuration of the residual nucleus is $(0p_\pi 0h_\pi 0p_\nu 1h_\nu)$ in this reaction, the energy spectra at forward angles are proportional to the single-particle density $\omega(0p_\pi 0h_\pi 0p_\nu 1h_\nu)$. As seen from Fig. 7,

these densities produce rather flat spectral shapes (with the exception of energies close to and/or below the Coulomb barrier), what is in agreement with [23]. The spectra of the $(\alpha, {}^3\text{H})$ reaction are proportional to $\omega(1p_\pi 0h_\pi 0p_\nu 0h_\nu) = g_\pi$ and they are limited by the energy of the neutron bound states. Thus the $({}^3\text{He}, \alpha)$ reaction serves to demonstrate differences between the densities $\omega(0p_\pi 0h_\pi 0p_\nu 1h_\nu)$ and $\omega(0p_\pi 0h_\pi 1p_\nu 1h_\nu)$, which is in contrary to the formalism of [23]. This difference can be understood, if one remembers that maximal energy that can be transferred to the hole degree of freedom cannot exceed the depth of the nuclear potential well $V = 38$ MeV [24].

Based on above mentioned features of experimental spectra, we suggest the following expression for the emission rates from unbound states, including formation of complex particles:

$$W_b(p, h, \varepsilon) = \frac{2s_b + 1}{\pi^2 \hbar^3} \mu_b \varepsilon \sigma_{\text{inv}}(\varepsilon_b) R_b(p) \frac{\omega^{(b)}(p - A_b, h, U)}{\omega^{(u)}(p, h, E)} \times \sum_{i=1}^{A_b} \gamma_b^{(i)} \frac{\Omega^{(iu)}(A_b, 0, E - U)}{g_b}, \quad (6)$$

where we have assumed that there is a different probability of clusterization in multiply unbound states, i.e. the states where more than one particle is unbound. Here, we keep the assumption (4) that the emission occurs from unbound states only. The first factor of the product

$$\omega^{(b)}(p - A_b, h, U) \times \sum_{i=1}^{A_b} \gamma_b^{(i)} \frac{\Omega^{(iu)}(A_b, 0, E - U)}{g_b} \quad (7)$$

ensures that residual nucleus will remain in a bound state, as it follows from the above analysis of the measured spectra, whereas the second one is due to the fact that emitted complex particles are formed in unbound states.

The density of states containing exactly i unbound particles $\Omega^{(iu)}(p, h, E)$ is given by

$$\Omega^{(iu)}(p, h, E) = \omega^{(iu)}(p, h, E) - \omega^{((i+1)u)}(p, h, E). \quad (8)$$

Here, $\omega^{(iu)}(p, h, E)$ is the density of states containing at least i unbound particles. With the help of formalism described in [11, 12], one can get ²

$$\omega^{(iu)}(p, h, E) = \omega(p, h, E) \times \frac{\int_{iS}^E \omega(i, 0, e) \omega(p - i, h, E - e) de}{\int_0^E \omega(i, 0, e) \omega(p - i, h, E - e) de}, \quad (9)$$

which results in

$$\omega^{(iu)}(p, h, E) = \frac{g_p^i(p) g_u^{n-i}(p)}{i!(p-i)! h!(n-1)!} E_u^{(n-1)} F_i(p), \quad (10)$$

with

$$E_u = E - C_{p-i, h} - iS. \quad (11)$$

Here, $C_{p-i, h}$ is correction on Pauli exclusion principle as defined in [11], S is separation energy of unbound states, and g_p and g_u are the single-particle state densities defined in [12].

²In fact, the form of the equation given here (as well as in [11, 12]) is not strictly valid if one considers the influence of the Pauli principle [25]. However, it leads to sufficiently good approximate resulting densities.

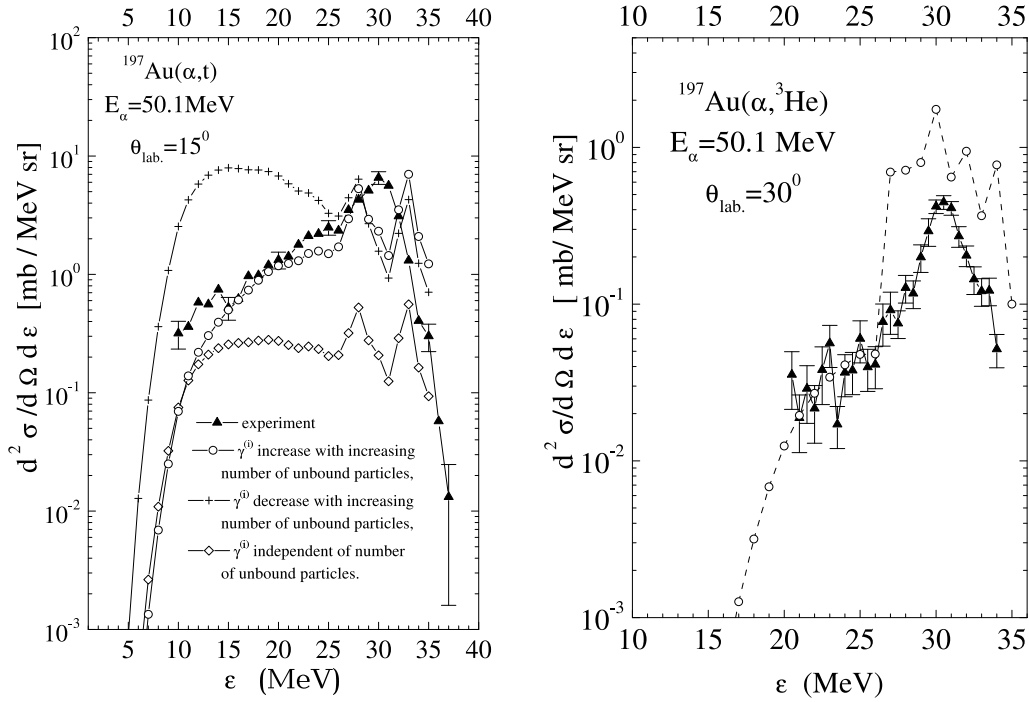


Fig. 8. Calculation of triton (left) and ${}^3\text{He}$ (right) spectra from $\alpha + {}^{197}\text{Au}$ according to Eq. (6) using different assumptions on the $\gamma^{(i)}$ for unbound particles compared to the data.

One can see that (10) is a generalization of the density of unbound states containing at least one unbound particle [11]. The correction factor $F_i(p)$ for the multiply unbound states is

$$F_i(p) = \binom{p}{i}^{-1} \sum_{k=i}^p \sum_{j=0}^h (-1)^{k+j+i} \binom{p}{k} \binom{h}{j} \mathcal{F}_{kj}^{(i)}, \quad (12)$$

where

$$\mathcal{F}_{kj}^{(i)} = \left[\frac{E - kS - jV}{E - iS} \right]^{n-1} \Theta(E - kS - jV). \quad (13)$$

The density of bound states $\omega^{(u)}(p, h, E)$ used in Eq. (6) is defined analogically [11]

$$\omega^{(b)}(p, h, E) = \omega(p, h, E) - \omega^{(u)}(p, h, E) \quad (14)$$

The dependence of the $\gamma^{(i)}$ parameters on the number of unbound particles i is not known *a priori*, unfortunately. Therefore, we have done calculations under three different assumptions on the $\gamma^{(i)}$ behaviour, namely:

i) $\gamma^{(i)}$ increases with the number of unbound particles,

- ii) $\gamma^{(i)}$ decreases with the number of unbound particles,
- iii) $\gamma^{(i)}$ is independent of the number of unbound particles.

The results of our calculations are presented in Fig. 8 for both the reactions. Thus, one can see that most adequate to experimental data is assumption *i*) about increasing clusterization probabilities with the number of unbound particles in initial states. It means that in the case of reactions induced with complex particles, different classes of unbound states are populated initially. They are ordered by their number of unbound particles, that is similar to the break-up of incident particle in initial state. Unfortunately, the population probabilities of such initial multiple unbound states are still undefined, and consequently one can consider the proposed expression (6) as only one of possible approaches to get the description of emitted particle spectra in reactions induced with complex particles in the framework of exciton model of pre-equilibrium decay.

4 Conclusions

The proposed formalism describes the (α, t) and $(\alpha, {}^3\text{He})$ reactions if we assume that the clusterization factor $\gamma^{(i)}$ increases with the number of unbound particles i . This feature is very similar to the interpretation of inelastic deuteron break-up process suggested many years ago [8]. In other words, we can get a description within the frame of the exciton model of reactions with complex particles as process of subsequent formation and population and decay of states differed by number of bound and unbound exciton particles, or as a process of multistep dissociation of incident particle from doorway (initial) configurations. Such a process has not been considered within the frame of the exciton model before, but the combined analysis of measured (α, t) and $(\alpha, {}^3\text{He})$ reactions clearly shows its existence and important role in relaxation process.

References

- [1] J. Bisplinghoff, J. Ernst, R. Löhr, T. Meyer-Kuckuk, P. Meyer: *Nucl. Phys. A* **269** (1976) 147
- [2] H.H. Bissem, R. Georgi, W. Scobel: *Phys. Rev. C* **22** (1980) 1468
- [3] N.T. Burtebaev, A.D. Duysebaev, G.N. Ivanov, V.I. Kanashevitch, V.A. Lichman: Report No. 5-83 (1983), INP Acad. Sci. Kaz. SSR, p. 74 (in Russian)
- [4] H. Feshbach, A. Kerman, S. Koonin: *Ann. Phys.* **125** (1980) 429
- [5] T. Tamura, T. Udagawa, H. Lenske: *Phys. Rev. C* **26** (1982) 379
- [6] P. Demetriou, A. Marcinkowski, P.E. Hodgson: *Nucl. Phys. A* **596** (1996) 67
- [7] G. Arbanas, M.B. Chadwick, F.S. Dietrich, A.K. Kerman: *Phys. Rev. C* **51** (1995) 1078
- [8] J. Kleinfeller, J. Bisplinghoff, J. Ernst, T. Mayer-Kuckuk, G. Baur, B. Hoffmann, R. Shyam, F. Rösel, D. Trautmann: *Nucl. Phys. A* **370** (1981) 205
- [9] J. Bisplinghoff: *Phys. Rev. C* **50** (1994) 1611
- [10] E. Běták: in *ICNRP '99, Proc. Second International Conf. Nuclear and Radiation Physics, Almaty 1999*, vol. 1, edited by K.K. Kadyrzhanov, Inst. Nucl. Phys. NNC RK, Almaty, 1999, p. 55; and the references therein
- [11] C. Kalbach: *Phys. Rev. C* **24** (1981) 819
- [12] C. Kalbach: *Phys. Rev. C* **23** (1981) 124
- [13] P. Obložinský: *Nucl. Phys. A* **453** (1986) 127

- [14] J.R. Wu, C.C. Chang, H.D. Holmgren: *Phys. Rev. C* **19** (1979) 659
- [15] N. Matsuoka, A. Shimizu, K. Hosono, T. Saito, M. Kondo, H. Sakaguchi, Y. Toba, A. Goto, F. Ohtani, N. Nakanishi: *Nucl. Phys. A* **311** (1978) 173
- [16] A.M. Blechman, A.D. Duysebaev, V.I. Kanashevich: *Yad. Fiz. (Russian J. Nucl. Phys.)* **56** (1993) 135
- [17] A. Gilbert, A.G.W. Cameron: *Can. J. Phys.* **43** (1965) 1446
- [18] P. Obložinský, I. Ribanský: *Izv. AN SSSR, Ser. Fiz. [Bull. Acad. Sci. USSR, Phys. Ser.]* **39** (1975) 2073 (in Russian)
- [19] G. Mantzouranis, H.A. Weidenmüller, D. Agassi: *Z. Phys. A* **276** (1976) 145
- [20] R. Perry, A. Nadasen, D.L. Hendrie, P.G. Roos, N.S. Chant: *Phys. Rev. C* **24** (1981) 1471
- [21] A.D. Duysebaev, F.A. Zhivopishev, V.I. Kanashevich, E.J. Käbin, V.A. Lichman, V.G. Sukharevskii, V.A. Khaimin: *Izv. AN SSSR, Ser. Fiz. [Bull. Acad. Sci. USSR, Phys. Ser.]* **41** (1977) 2132 (in Russian)
- [22] V.V. Adodin, A.M. Blechman, A.D. Duysebaev, N. Burtebaev, G.N. Ivanov, V.I. Kanashevich: *Thez. of Rep. 36th Conference on Structure of Atomic Nucleus*, St. Petersburg, Nauka Publ. Co., 1986, p. 342 (in Russian)
- [23] F.C. Williams, Jr.: *Nucl. Phys. A* **166** (1971) 231
- [24] E. Běták, J. Dobeš: *Z. Phys. A* **279** (1976) 319
- [25] J. Dobeš, E. Běták: *Nucl. Phys. A* **272** (1976) 353